Journal of Cellular Physiology



# Heat Stress Modulates Both Anabolic and Catabolic Signaling Pathways Preventing Dexamethasone-Induced Muscle Atrophy In Vitro

WAKAKO TSUCHIDA,[1,2] MASAHIRO IWATA,[1,2] TAKAYUKI AKIMOTO,[3] SHINGO MATSUO,[1,2] YUJI ASAI,[1] AND SHIGEYUKI SUZUKI[2]*

[1]*Department of Rehabilitation, Faculty of Health Sciences, Nihon Fukushi University, Handa, Aichi, Japan*

[2]*Program in Physical and Occupational Therapy, Graduate School of Medicine, Nagoya University, Nagoya, Aichi, Japan*

[3]*Faculty of Sport Sciences, Waseda University, Tokorozawa, Saitama, Japan*

It is generally recognized that synthetic glucocorticoids induce skeletal muscle weakness, and endogenous glucocorticoid levels increase in patients with muscle atrophy. It is reported that heat stress attenuates glucocorticoid-induced muscle atrophy; however, the mechanisms involved are unknown. Therefore, we examined the mechanisms underlying the effects of heat stress against glucocorticoid-induced muscle atrophy using C2C12 myotubes in vitro, focusing on expression of key molecules and signaling pathways involved in regulating protein synthesis and degradation. The synthetic glucocorticoid dexamethasone decreased myotube diameter and protein content, and heat stress prevented the morphological and biochemical glucocorticoid effects. Heat stress also attenuated increases in mRNAs of regulated in development and DNA damage responses 1 (REDD1) and Kruppel-like factor 15 (KLF15). Heat stress recovered the dexamethasone-induced inhibition of PI3K/Akt signaling. These data suggest that changes in anabolic and catabolic signals are involved in heat stress-induced protection against glucocorticoid-induced muscle atrophy. These results have a potentially broad clinical impact because elevated glucocorticoid levels are implicated in a wide range of diseases associated with muscle wasting.

J. Cell. Physiol. 232: 650–664, 2017. © 2016 The Authors. *Journal of Cellular Physiology* published by Wiley Periodicals, Inc.

Skeletal muscle has a crucial role in movement, breathing, and glucose homeostasis, as well as energy homeostasis and thermogenesis. Various chronic diseases result in reduced skeletal muscle mass (muscle atrophy), which compromises patient quality of life. Therefore, preventing and attenuating skeletal muscle atrophy is an important clinical goal.

Glucocorticoids (GC) are steroid hormones with wide-ranging regulatory effects on development and metabolism (Revollo and Cidlowski, 2009) as well as potent anti-inflammatory and immunosuppressive activities, and new GC have been synthesized for therapeutic use. However, GC induce adverse effects including hyperglycemia, weight gain, hypertension, osteoporosis, depression, decreased immunological function, and skeletal muscle weakness (Ramamoorthy and Cidlowski, 2013). Many pathological conditions characterized by muscle weakness, including sepsis, cachexia, starvation, metabolic acidosis, and severe insulinopenia, are associated with increased circulating GC levels (Wing and Goldberg, 1993; Tiao et al., 1996; Hu et al., 2009; Braun et al., 2011, 2013), suggesting they might be involved in muscle atrophy.

GC-induced muscle atrophy results from decreased the rate of protein synthesis and increased the rate of protein breakdown (Tomas et al., 1979; Goldberg et al., 1980; Lofberg et al., 2002). GC decrease the rate of protein synthesis in skeletal muscle by enhancing the transcription of "regulated in development and DNA damage responses 1" (REDD1) and "Kruppel-like factor 15" (KLF15) that represses mammalian target of rapamycin complex 1 (mTORC1) (Shimizu et al., 2011). In addition, GC mediate anti-anabolic actions by inhibiting phosphatidylinositol 3-kinase (PI3K)/Akt-dependent mTORC1 signaling (Kuo et al., 2012). Phosphorylation of glycogen synthase kinase 3β (GSK3β) by Akt may also be involved in the anti-anabolic effect of GC because dephosphorylation of GSK3β suppresses protein synthesis (Proud and Denton, 1997). GC-induced muscle atrophy also involves increased muscle proteolysis signaling, especially muscle RING finger 1 (MuRF1) and Atrogin-1/muscle atrophy F-box (MAFbx), both muscle-specific E3 ubiquitin ligases (Bodine et al., 2001; Sacheck et al., 2004; Wada et al., 2011) that target several muscle regulatory and myofibrillar proteins for degradation via the ubiquitin-proteasome system (UPS). In



Conflicts of interest: The authors declare that they have no competing interests.

Contract grant sponsor: Japan Society for the Promotion of Science (JSPS);
Contract grant numbers: 26870691, 26350639.

*Correspondence to: Shigeyuki Suzuki, Program in Physical and Occupational Therapy, Graduate School of Medicine, Nagoya University, 1-1-20 Daikominami, Higashi-ku, Nagoya, Aichi 461-8673, Japan. E-mail: suzuki@met.nagoya-u.ac.jp

Manuscript Received: 21 February 2016
Manuscript Accepted: 19 September 2016

Accepted manuscript online in Wiley Online Library (wileyonlinelibrary.com): 20 September 2016.
DOI: 10.1002/jcp.25609

skeletal muscle, MuRF1 and Atrogin-1 are transcriptionally activated by dephosphorylation of forkhead box O1 and 3a (FoxO1 and FoxO3a) (Kamei et al., 2004; Sandri et al., 2004; Senf et al., 2008; Waddell et al., 2008). Activation of PI3K/Akt signaling rescued GC-mediated atrophy through the phosphorylation and inactivation of FoxO1/FoxO3a (Sandri et al., 2004; Stitt et al., 2004; Latres et al., 2005). KLF15 also has catabolic activity by trans-activations of MuRF1 and Atrogin-1 (Shimizu et al., 2011).

Heat stress is widely used as an adjuvant to physical rehabilitation for controlling pain and relieving muscle spasms (Lehmann et al., 1974). Recently, the benefits of heat stress for muscle atrophy under various conditions were described (Naito et al., 2000; Luo et al., 2001; Selsby and Dodd, 2005; Ichinoseki-Sekine et al., 2014; Morimoto et al., 2015; Tamura et al., 2015; Yoshihara et al., 2015). Heat stress attenuated GC-induced muscle atrophy in rats (Morimoto et al., 2015) and prevented GC-induced degradation of proteins in cultured L6 myotubes (Luo et al., 2001). However, the mechanisms of heat stress-induced suppression of GC-induced muscle atrophy remain unclear.

In this study, we examined the mechanisms involved in the preventive effect of heat stress for GC-induced muscle atrophy, focusing on anabolic and catabolic signaling pathways. We used a well-established in vitro system of cultured C2C12 myotubes to model skeletal muscle atrophy. Heat stress prevented the deleterious effects of GC by modifying REDD1 and KLF15 expression and recovering GC-affected PI3K/Akt signaling. Therefore, heat stress modulates both anabolic and catabolic signaling pathways in skeletal muscle.

## Materials and Methods

### Cell culture

The murine skeletal muscle cell line C2C12 was obtained from the European Collection of Cell Cultures (Salisbury, UK), and maintained as described previously (Iwata et al., 2009). C2C12 myoblasts were cultured at $5 \times 10^3$ cells/cm$^2$ on type I collagen coated 60-mm dishes (Japan BD, Tokyo, Japan) with 4 ml growth medium consisting of high glucose (4.5 g/l) Dulbecco's Modified Eagle's Medium (DMEM, Sigma–Aldrich, St. Louis, MO) containing 15% (v/v) heat-inactivated fetal bovine serum (Gibco, Carlsbad, CA) and antibiotics (100 U/ml penicillin and 100 μg/ml streptomycin, Gibco) for approximately 48 h in a water-jacketed humidified incubator (MCO-18AIC, Sanyo, Osaka, Japan) equilibrated with 5% $CO_2$ and 95% air, at 37°C, until the myoblasts reached about 90% confluence. To induce spontaneous differentiation by growth factor withdrawal (Yaffe and Saxel, 1977), growth medium was replaced with differentiation medium consisting of low glucose (1 g/l) DMEM containing 2% (v/v) heat-inactivated horse serum (Gibco). In this medium, the myoblasts fused to form elongated, multi-nucleated myotubes. After 5 days, when approximately 90% of the cells had fused into myotubes, cultures were treated with 10 μM cytosine β-D-arabinofuranoside hydrochloride (Ara-C; C6645, Sigma–Aldrich) for 48 h to remove dividing myoblasts. Myotubes reached a well-differentiated state showing cross-striation, with a few myotubes displaying spontaneous contractions. Medium was replenished every 48 h during the 5-day differentiation, then once every 24 h after the addition of Ara-C and again 2 h before heat treatment. To induce muscle atrophy in vitro, cells were treated with the synthetic GC, dexamethasone (Dex; D2915, Sigma–Aldrich) in differentiation medium for the indicated times and concentrations. In some experiments, cells were treated with the PI3K inhibitor wortmannin (681675; Merck Millipore, Billerica, MA) 2 h before heat treatment. Wortmannin was maintained throughout the experiment. Wortmannin was prepared in dimethyl sulfoxide (DMSO) and diluted in differentiation medium to the indicated concentrations. The final concentration of DMSO never exceeded 0.1% (v/v). Control cells were treated with DMSO alone. After treatments, cells were harvested in appropriate buffers for various analyses or were fixed for morphological analysis.

### Heat treatment

Heat stress was performed as previously described with modifications (Welc et al., 2012). C2C12 myotubes were maintained at 37°C or were treated in a water-jacketed humidified incubator (MCO-18AIC, Sanyo) preset to an elevated temperature (41°C or, only where indicated, other temperatures) and then, after 60 min exposure to the higher temperature, were returned to the original 37°C incubator. Once cells were placed in an incubator at 41°C, it required about 42.5 min for the temperature of medium in the dishes to reach the desired experimental temperature (Supplemental Fig. S1A). Control cells were maintained at 37°C for the entire experiment. After heat treatment, medium in the cells returned to 37°C after 37.5 min. We previously reported that 72-kDa heat shock protein (Hsp72) protein expression in C2C12 myotubes was significantly increased after 4–24 h of heat treatment, peaking at 6 h (Tsuchida et al., 2012). Thus, in the current study, a 1-h heat treatment period was used, beginning at 7 h prior to Dex treatment.

### Myotube morphological analysis

After treating C2C12 myotubes for 12 or 24 h with Dex, the myotubes were fixed in methanol and stained in Giemsa (109204, Merck Millipore) according to the manufacturer's instructions. Images were captured at 100× magnification under a phase contrast microscope (Axio Observer A1, Carl Zeiss, Oberkochen, Germany) with a microscopic camera system (AxioCamHRm, Carl Zeiss). Average diameters of at least 50 myotubes were measured for each condition at three locations 50 μm apart along the length of the myotubes using image editing software (Adobe Photoshop CS5, Adobe Systems, CA) as previously described (Stitt et al., 2004). Measurements were conducted in a blinded fashion on coded images (control, Dex-, or heat stress + Dex-treated myotubes) of myotubes from each group.

### Protein isolation

After the indicated treatments, C2C12 myotubes were washed twice with ice-cold phosphate buffered saline (PBS, Sigma–Aldrich) and were harvested with cell scrapers in whole-cell lysate buffer composed of 200 μl ice-cold RIPA buffer (R0278, Sigma–Aldrich) containing 10% (v/v) protease inhibitor cocktail (P8340, Sigma–Aldrich) and 1% (v/v) phosphatase inhibitor cocktail (524625, Calbiochem, Darmstadt, Germany). Cell lysates were treated with an ultrasonic disintegrator (Bioruptor UCD-200T, Cosmo Bio, Tokyo, Japan) and then centrifuged at 8,000*g* for 10 min at 4 °C. The supernatants were collected as cell extracts. The total protein content in each cell extract was measured using the BCA protein assay kit (23225, Thermo Fisher Scientific, Waltham, MA) according to the manufacturer's instructions.

### Western blot analysis

Each extract was adjusted to a concentration of 2 μg protein per μl with an appropriate volume of RIPA buffer for SDS–PAGE. These samples were each added to an equal volume of EzApply (Atto, Tokyo, Japan) containing 100 mM Tris–HCl buffer (pH 8.8), 2% SDS, 20% sucrose, 0.06% bromophenol blue and 100 mM DTT, and heated at 95°C for 5 min. For SDS–PAGE, samples containing 10–30 μl protein were loaded per lane and separated on precast polyacrylamide gradient (7.5–12%, Bio-Rad, Hercules, CA) gels at 200 V for 30 min. Proteins were then transferred from the gel to 0.2-μm polyvinylidene difluoride membranes (Bio-Rad) by electro-blotting at a constant current

of 1.3 A for 7 min using a rapid transfer system (Trans-Blot Turbo, Bio-Rad). After transfer, western blot analysis was performed with a protein detection system (SNAP i.d. 2.0, Merck Millipore). The blots were blocked with 0.5% (w/v) nonfat dried milk or 1% (w/v) bovine serum albumin diluted in Tris-buffered saline containing 0.1% (v/v) Tween 20 (TBS-T), to block nonspecific reactions, and then incubated overnight at 4°C with the indicated primary antibodies. These antibodies were directed against Hsp72 (ADI-SPA-812, Enzo Life Sciences, Farmingdale, NY), phosphorylated Akt (Thr308; #2965, Cell Signaling Technology, Danvers, MA), Akt (#4691, Cell Signaling Technology), phosphorylated p70 ribosomal protein S6 kinase 1 (p70S6K1) (Thr389; #9206, Cell Signaling Technology), p70S6K1 (#2708, Cell Signaling Technology), phosphorylated GSK3β (Ser9; #5558, Cell Signaling Technology), GSK3β (#9832, Cell Signaling Technology), phosphorylated mitogen-activated protein kinase kinase 1/2 (MEK1/2) (Ser217/221; #9154, Cell Signaling Technology), MEK1/2 (#9122, Cell Signaling Technology), phosphorylated extracellular signal-regulated kinase 1/2 (ERK1/2) (Thr202/Tyr204; #4370, Cell Signaling Technology), ERK1/2 (#4696, Cell Signaling Technology), phosphorylated FoxO1 (Thr256; #9461, Cell Signaling Technology), FoxO1 (#2880, Cell Signaling Technology), phosphorylated FoxO3a (Ser253; ab47285, Abcam, Cambridge, MA), FoxO3a (#2497, Cell Signaling Technology), total myosin heavy chain (MyHC) (MF20, Developmental Studies Hybridoma Bank, Iowa, IA), MyHC fast (MyHC-f) (M4276, Sigma–Aldrich), and β-actin (#5125, Cell Signaling Technology). The blots were washed, incubated with the respective secondary antibodies, and washed again. The immunostained bands were visualized using the ECL Prime Western Blotting Detection System (RPN2232, GE Healthcare Japan, Tokyo, Japan) according to the manufacturer's instructions. Illumination patterns were measured using a high sensitivity cooled CCD camera (Light Capture II, Atto) to obtain an image of the target protein bands. Subsequent quantification of band images was performed using image analysis software (CS analyzer 3.0, Atto).

### RNA isolation and assessment of mRNA expression by real-time quantitative RT-PCR

C2C12 myotubes were washed twice with PBS and total RNA was isolated using the PureLink® RNA Mini Kit (Life Technologies, Grand Island, NY) according to the manufacturer's instructions. RNA concentrations were measured using a Nanodrop ND-1000 UV-Vis spectrophotometer (Thermo Scientific, Wilmington, DE). Next, total RNA was reverse transcribed into cDNA using the High-Capacity RNA-to-cDNA™ Kit (Life Technologies) and a 2,720 thermocycler (Life Technologies), according to the manufacturer's instructions. Quantitation of gene expression was determined by real-time quantitative reverse transcription PCR (qRT-PCR). qRT-PCR reactions contained 2 μl cDNA (50 μg/μl), 10 μl TaqMan Fast Advanced Master Mix (Life Technologies), and 1 μl primers. PCR reaction analysis was performed by a StepOnePlus Real-time PCR system (Life Technologies) using the ΔΔCt method. The primers were as follows: Hsp72 (Mm01159846_s1), REDD1 (Mm00512504_g1), REDD2 (Mm00513313_m1), KLF15 (Mm00517792_m1), FoxO1 (Mm00490672_m1), FoxO3a (Mm01185722_m1), Atrogin-1 (Mm00499523_m1), MuRF1 (Mm01185221_m1), and glyceraldehyde-3-phosphate dehydrogenase (GAPDH; Mm99999915_g1) by TaqMan Gene Expression Assays (Life Technologies). GAPDH was used as an endogenous control to normalize the samples.

### Statistical analysis

Statistical analyses were performed using SPSS version 15.0 (SPSS Inc., Chicago, IL). All values are presented as means ± standard deviation (SD). The data were analyzed using the Mann–Whitney *U*-test for comparisons between two conditions, the Kruskal–Wallis test followed by Steel's test for comparisons with controls, and the Steel–Dwass test for multiple comparisons. Differences between conditions were considered statistically significant at $P < 0.05$.

## Results

### Dex treatment induces C2C12 myotube atrophy

We examined the dose-dependent effects of Dex by assessing myotube diameter. Compared with untreated controls ($n = 55$, myotube diameter $18.7 \pm 4.5$ μm), fully differentiated C2C12 myotubes treated with Dex for 24 h showed a distinct atrophic phenotype (Fig. 1A), with a dose-dependent decrease in myotube diameter (Fig. 1B). In myotubes treated with Dex 0.01 μM, there were no significant effects, although a trend toward a 2% decrease in diameter ($n = 54$, $18.3 \pm 4.9$ μm), with a similar trend of a 10% decrease with 0.1 μM Dex ($n = 53$, $16.8 \pm 4.2$ μm) was observed. Myotube diameters were significantly decreased by 18% with 1 μM ($n = 51$, $15.4 \pm 3.1$ μm) and by 23% with 10 μM ($n = 54$, $14.4 \pm 3.5$ μm) or 100 μM ($n = 54$, $14.5 \pm 3.5$ μm) Dex ($P < 0.05$) (Fig. 1B). Based on this, 10 μM Dex was used in subsequent experiments to induce atrophy in C2C12 myotubes.

Next, we examined the time dependence of the effect of Dex (10 μM) treatment on C2C12 myotube diameter. Compared with controls, the diameters of myotubes treated with Dex were unchanged at 12 h but showed a significant decrease of 24% at 24 h (Fig. 1C). Similar to its effect on diameter, Dex treatment significantly decreased the total protein content by 16% (Fig. 1D), MyHC-f content by 21% (Fig. 1E and F), and total MyHC content by 24% at 24 h, compared with controls (Fig. 1E and G), but had no effect at 12 h. Thus, the in vitro response of C2C12 myotubes to Dex recapitulated the in vivo response of skeletal muscle (Hickson and Davis, 1981; Ma et al., 2003; Clarke et al., 2007; Yamamoto et al., 2010). In addition, these data were consistent with previous studies reporting Dex decreased myotube diameter (Chromiak and Vandenburgh, 1992; Sandri et al., 2004; Stitt et al., 2004; Latres et al., 2005; Menconi et al., 2008; Kukreti et al., 2013), total protein (Chromiak and Vandenburgh, 1992; Sacheck et al., 2004; Stitt et al., 2004; Polge et al., 2011; Wada et al., 2011), and/or myofibrillar protein content (Chromiak and Vandenburgh, 1992; Clarke et al., 2007; Verhees et al., 2011) in vitro.

### Dex treatment increases REDD1, KLF15, FoxO1, FoxO3a, MuRF1, and Atrogin-1 mRNA expression in C2C12 myotubes

It was previously shown that REDD1, REDD2, and KLF15, upstream negative effectors of mTORC1 signaling, induced muscle atrophy via the inhibition of protein synthesis (Wang et al., 2006; Shimizu et al., 2011; Kelleher et al., 2013; Britto et al., 2014). Furthermore, the key muscle proteolysis factors, MuRF1 and Atrogin-1, were transcriptionally activated by KLF15, FoxO1, and FoxO3a in response to Dex (Kamei et al., 2004; Sandri et al., 2004; Waddell et al., 2008; Shimizu et al., 2011). Therefore, we assessed the mRNA expression of these regulatory factors in fully differentiated C2C12 myotubes undergoing Dex-induced skeletal muscle atrophy. REDD1 mRNA expression rapidly increased by 3.1-fold at 1 h, reached a peak of 3.6-fold increase at 3 h and gradually decreased at 6–24 h of Dex (10 μM) treatment (Fig. 2A). In contrast, REDD2 mRNA expression was unchanged throughout the entire Dex treatment period (Fig. 2B). KLF15 mRNA expression increased by 3.2- and 5.2-fold at 1 and 3 h, respectively, and reached a 6.3-fold peak at 6 h of Dex treatment (Fig. 2C). FoxO1 mRNA expression

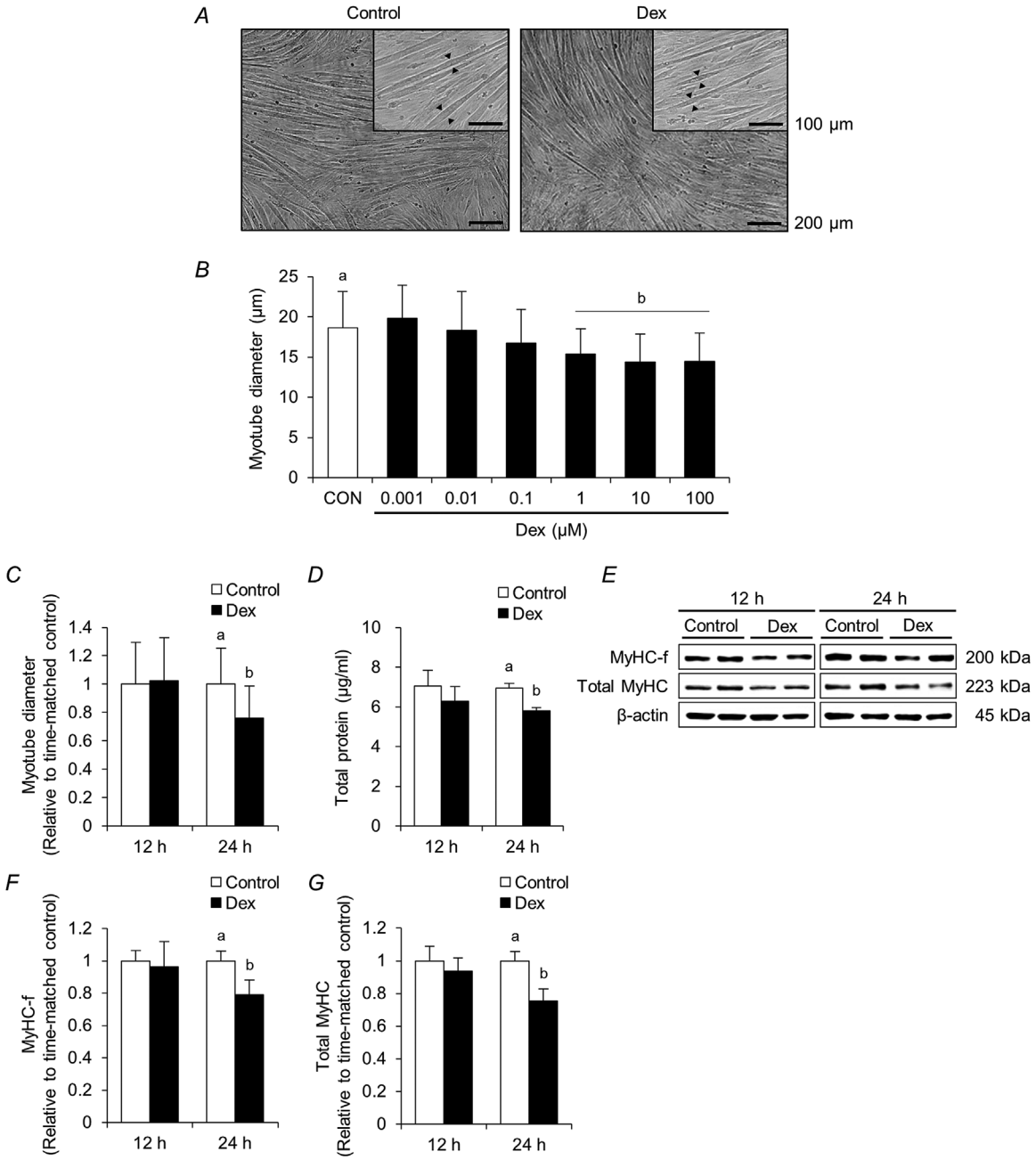


**Fig. 1. Dex treatment induces atrophic responses in C2C12 myotubes. Fully differentiated C2C12 myotubes were treated with the synthetic GC Dex. A: Representative images of C2C12 myotubes were acquired after 24 h treatment with 10 μM Dex. The scale bars represent 100 or 200 μm. B: The graph shows myotube diameters after 24 h Dex treatment at the indicated concentrations. Data are means ± SD (n ≥ 51 myotubes per condition). C: The graph shows myotube diameters in response to 10 μM Dex treatment for 12 or 24 h. Data are means ± SD (n ≥ 118 myotubes per condition), relative to the mean value of the control condition, which was set as 1. D: The graph shows total protein content in response to 10 μM Dex. Data are means ± SD (n = 3 dishes per condition). E–G: Effects of treatment with 10 μM Dex on MyHC-f and total MyHC content were measured by western blot. β-Actin was used as a protein loading control. MyHC-f and total MyHC content are expressed as means ± SD (n = 4 dishes per condition). a and b indicate significant differences among the designated groups ($P < 0.05$), where a > b.**

was increased by 1.2-fold, although this increase was observed only at 1 h of Dex treatment (Fig. 2D). FoxO3a mRNA expression increased by 1.3-fold at 1 h and reached a 2.0-fold peak at 3 h of Dex treatment (Fig. 2E). MuRF1 mRNA expression gradually increased by 1.2- and 1.6-fold at 1 and 3 h, respectively and reached a 2.0-fold peak at 6 h of Dex treatment (Fig. 2F). Atrogin-1 mRNA expression was not increased at 1 h, but rapidly increased to 1.7-fold at 3 h of Dex treatment, remaining stable at 1.7–1.8-fold at later time points (Fig. 2G). Thus, the peak expression of REDD1 was at 3 h of Dex treatment and this time point was used to investigate changes in the anabolic markers, REDD1, KLF15, Akt, p70S6K1, and GSK3β, during Dex-induced atrophy. We investigated gene expression at 3–12 h, and myotube

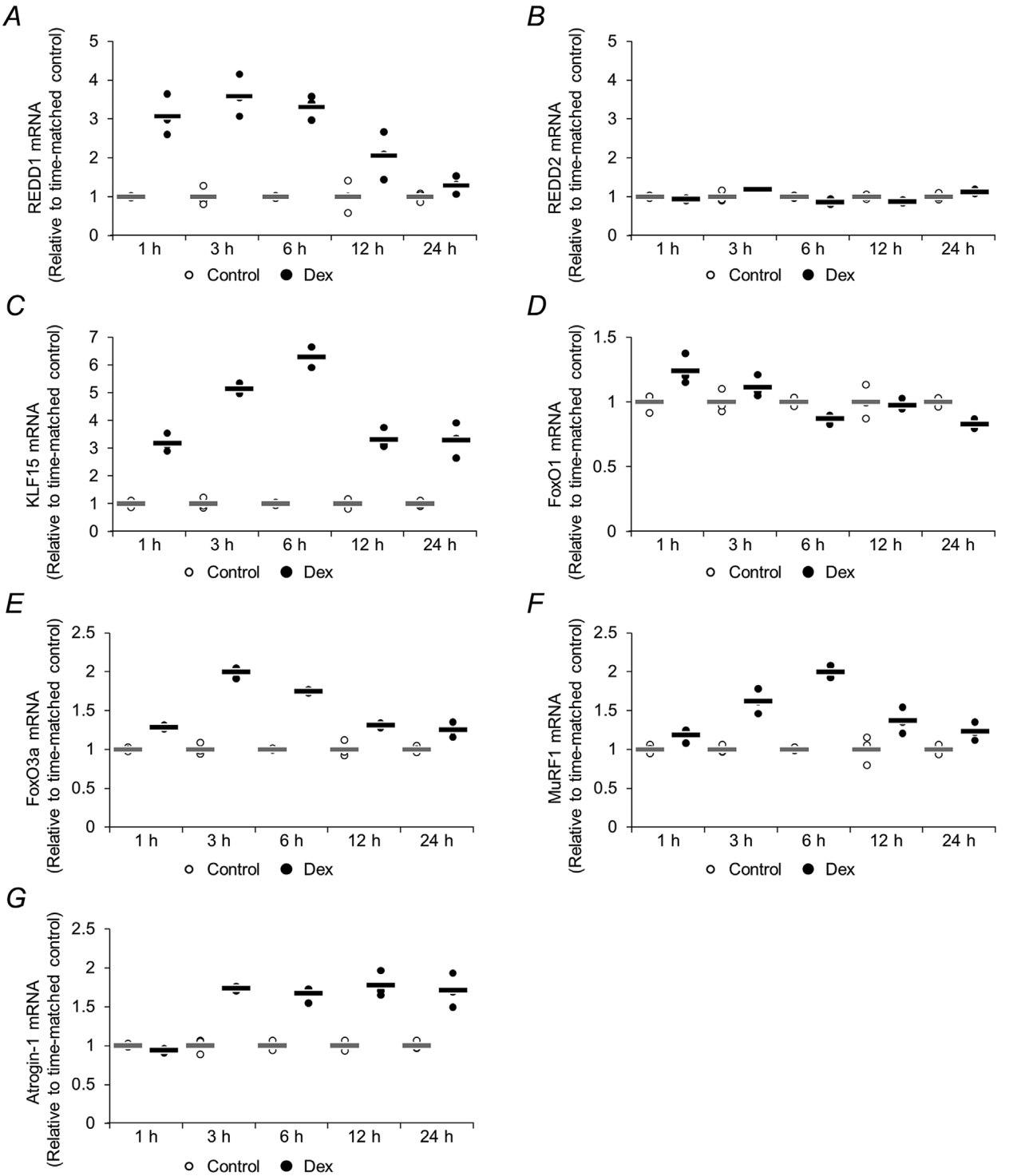


**Fig. 2. Time course of Dex effects on REDD1, REDD2, KLF15, FoxO1, FoxO3a, MuRF1, and Atrogin-1 mRNA expression in C2C12 myotubes. A–G: Fully differentiated C2C12 myotubes were treated with Dex (10 μM) for the indicated times. REDD1, REDD2, KLF15, FoxO1, FoxO3a, MuRF1, and Atrogin-1 mRNA expressions were measured by real-time quantitative RT-PCR (open circles, control; filled circles, Dex treated). Horizontal bars indicate mean values (n = 3 dishes per condition), relative to the mean value of the control condition that was set as 1.**

diameter/protein up to 24 h, because there is a temporal peak of gene expression before the physiological response occurs. The peak of changes in MuRF1 and Atrogin-1, both considered rate-limiting enzymes of UPS-mediated muscle protein breakdown, was at 6 h of Dex treatment. Therefore, we analyzed C2C12 myotubes at 6 h of Dex treatment to investigate changes in the catabolic markers, KLF15, Akt, FoxO, MuRF1, and Atrogin-1, during Dex-induced atrophy.

We next investigated how REDD1 and KLF15 expression was regulated during this process in more detail. Dex signals by binding to GC receptor (GR), which then translocates into the nucleus to regulate the expression of target genes (Kadmiel and Cidlowski, 2013). We investigated whether GR was involved in the Dex-mediated upregulation of REDD1 and KLF15 mRNA expression. When fully differentiated C2C12 myotubes were treated with a GR-specific antagonist RU486, Dex-induced increases in REDD1 and KLF15 mRNA expression were inhibited (Supplemental Fig. S2A and B), indicating REDD1 and KLF15 expression was mediated by the GR in Dex-induced atrophy.

### Heat stress suppresses Dex-induced muscle atrophy

In previous studies, heat stress attenuated the Dex-induced decrease in muscle fiber diameter of extensor digitorum longus muscle in vivo in rats (Morimoto et al., 2015) and suppressed Dex-induced muscle proteolysis in L6 myotubes in vitro (Luo et al., 2001). These effects were attributed to Hsp72 induced by heat stress. To investigate whether heat stress induced Hsp72 mRNA and protein expression under our experimental conditions, we exposed fully differentiated C2C12 myotubes to heat stress. Treating C2C12 myotubes at 39, 40, or 41°C increased Hsp72 mRNA expression by 1.5-, 3.5-, and 6.0-fold, respectively, when measured immediately after heat treatment. Hsp72 mRNA expression gradually decreased over time reaching control levels at 5 h after heat treatment (Supplemental Fig. S1B). Hsp72 protein expression was significantly increased by 2.2- and 4.7-fold at 39 and 41°C, respectively, at 6 h of heat treatment, compared with control myotubes maintained at 37°C (Supplemental Fig. S1C and D). Thus, heat stress-induced increases in Hsp72 mRNA and protein expression were temperature-dependent. Accordingly, heat stress at 41°C, which induced sufficient levels of Hsp72 expression, was used for subsequent experiments to investigate how heat stress influences Dex-induced atrophy in C2C12 myotubes. Fully differentiated C2C12 myotubes

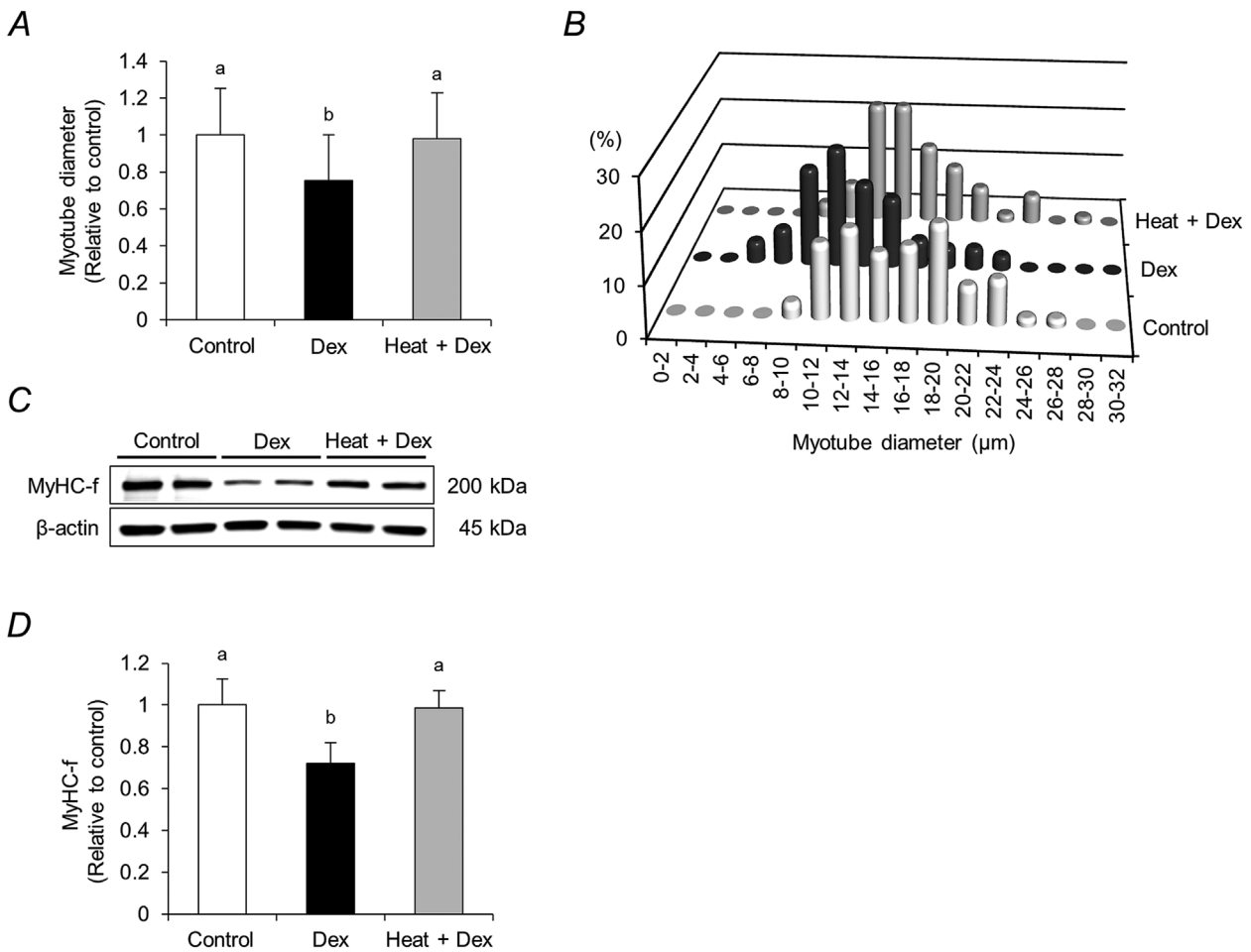


**Fig. 3. Heat stress suppresses Dex-induced decreases in myotube diameter and MyHC-f content. Fully differentiated C2C12 myotubes were exposed to heating (at 41°C for 60 min) 6 h prior to adding 10 μM Dex and treating for 24 h. The experiment was conducted using three conditions in which C2C12 myotubes were untreated (control), treated with 10 μM Dex (Dex), or exposed to heating and then treated with 10 μM Dex (Heat + Dex). A: The graph shows average myotube diameters under the three conditions. Data are means ± SD ($n \geq 69$ myotubes per condition), relative to the mean value of the control condition which was set to 1. a and b indicate significant differences among the designated groups ($P < 0.01$). B: Frequency histogram showing distribution of myotube diameters. C–D: MyHC-f content measured by western blotting with β-actin as a protein loading control. MyHC-f content is expressed as mean ± SD ($n = 7$ dishes per condition). a and b indicate significant differences among the designated groups ($P < 0.01$), where a > b.**

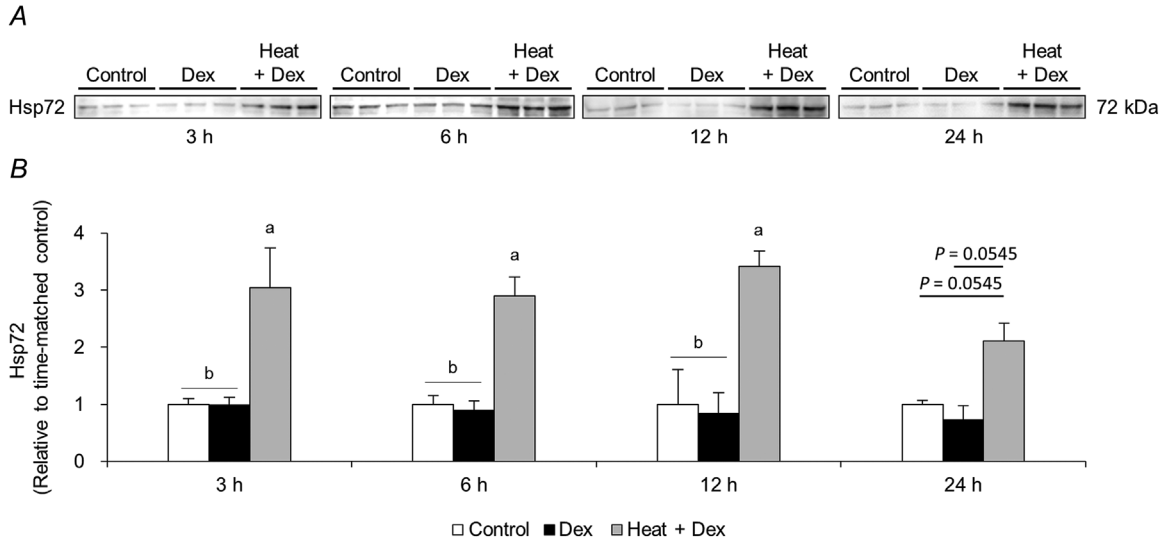


**Fig. 4. Heat stress increases Hsp72 protein expression in C2C12 myotubes during Dex treatment. A and B: Fully differentiated C2C12 myotubes were exposed to heating (at 41°C for 60 min) 6 h prior to 10 μM Dex treatment for 3, 6, 12, and 24 h, as indicated. The experiment was conducted using three conditions, control, Dex, and Heat + Dex conditions, as described for Figure 3. Hsp72 protein levels were measured by western blotting and are expressed as means ± SD (n = 4–6 dishes per condition), relative to the mean value of the control condition that was set as 1. a and b indicate significant differences among the designated groups ($P < 0.05$), where a > b.**

exposed to heat stress (at 41°C for 60 min) ending 6 h prior to treatment with Dex (10 μM) for 24 h had a 25% decrease in diameter when maintained at normal temperature, but this was abolished when subjected to heat stress (Fig. 3A). Compared with untreated controls, C2C12 myotubes treated with Dex had a lower percentage of large myotubes (>20 μm) and a higher percentage of small myotubes (>10 μm) (Fig. 3B). Both Dex-induced effects were suppressed in myotubes subjected to heat stress. Furthermore, a 28% loss of MyHC-f content in C2C12 myotubes induced by Dex treatment was also abolished by heat stress (Fig. 3C and D). Therefore, heat stress suppressed Dex-induced decreases in both myotube diameter and myofibrillar protein content. In addition, C2C12 myotubes exposed to heat stress (at 41°C for 60 min) 6 h prior to Dex treatment showed Hsp72 protein expression was increased 3.0-, 2.9-, 3.4-, and 2.1-fold at 3, 6, 12, and 24 h, respectively, of Dex treatment (Fig. 4A and B) indicating that heating at 41°C for 60 min induced a sustained increase in Hsp72 protein expression throughout the period of Dex treatment in C2C12 myotubes.

### Heat stress suppresses Dex-induced increases in REDD1 and KLF15 mRNA expression and decreases in phosphorylated Akt, p70S6K1, and GSK3β protein levels in C2C12 myotubes

To elucidate the effects of heat stress on Dex-mediated inhibition of anabolic pathways, we measured mRNA expression of REDD1 and KLF15 (Shimizu et al., 2011; Britto et al., 2014), in C2C12 myotubes treated with Dex (10 μM) for 3 h. Dex-treated C2C12 myotubes showed a 3.6-fold increase in REDD1 mRNA and a 4.8-fold increase in KLF15 mRNA expression, both of which were blunted by heat stress (Fig. 5A and B). We next examined Akt phosphorylated on Thr308, because REDD1-mediated inhibition of mTORC1 involves Akt dephosphorylation at this site (Britto et al., 2014). Dex treatment resulted in a 30% decrease in phosphorylated Akt on Thr308 in myotubes with no change in total Akt protein (Fig. 5C–E). This effect was inhibited by heat stress (Fig. 5C–E). We also examined mTORC1 activity by evaluating phosphorylation of p70S6K1 at the mTOR-specific site Thr389 (Brown et al., 1995; Brunn et al., 1997). Similar to the observations with Akt, Dex treatment resulted in a 29% decrease in phosphorylated p70S6K1 at Thr389, with no change in total p70S6K1 protein, and heat stress prevented this effect (Fig. 5C, F, and G). Because Akt reduces GSK3β kinase activity through the phosphorylation of Ser9 (Manning and Cantley, 2007) and increases mRNA translation and protein synthesis (Proud and Denton, 1997), we analyzed phosphorylated GSK3β levels in Dex-treated C2C12 myotubes, with/without heat stress. We observed a 34% decrease in phosphorylated GSK3β on Ser9 after Dex treatment, with no change in total GSK3β protein (Fig. 5C, H, and I). This effect was inhibited by heat stress (Fig. 5C, H, and I).

### Dex treatment and heat stress do not alter MEK1/2 and ERK1/2 signals in C2C12 myotubes

The MEK/ERK signaling pathway enhanced protein synthesis by regulating ribosomal RNA gene expression (Stefanovsky et al., 2006) and might contribute to the maintenance of skeletal muscle mass by modulating Akt signaling (Shi et al., 2009). Therefore, we examined the phosphorylation states of MEK1/2 at Ser217/221 sites and the downstream effector ERK1/2 at Thr202/Tyr204 sites in our atrophy model. Treatment of C2C12 myotubes with Dex for 3 h did not affect the levels of phosphorylated and total MEK1/2 and ERK1/2 (Fig. 6A–E) consistent with a previous study showing Dex had no effect on the signaling pathway (Gwag et al., 2013). Similarly, heat stress did not alter the levels of phosphorylated and total MEK1/2 and ERK1/2 in Dex-treated C2C12 myotubes (Fig. 6A–E), suggesting the MEK/ERK signaling pathway is not involved in the Dex-induced inhibition of protein synthesis and heat stress-induced anti-atrophic effects under the present experimental conditions.

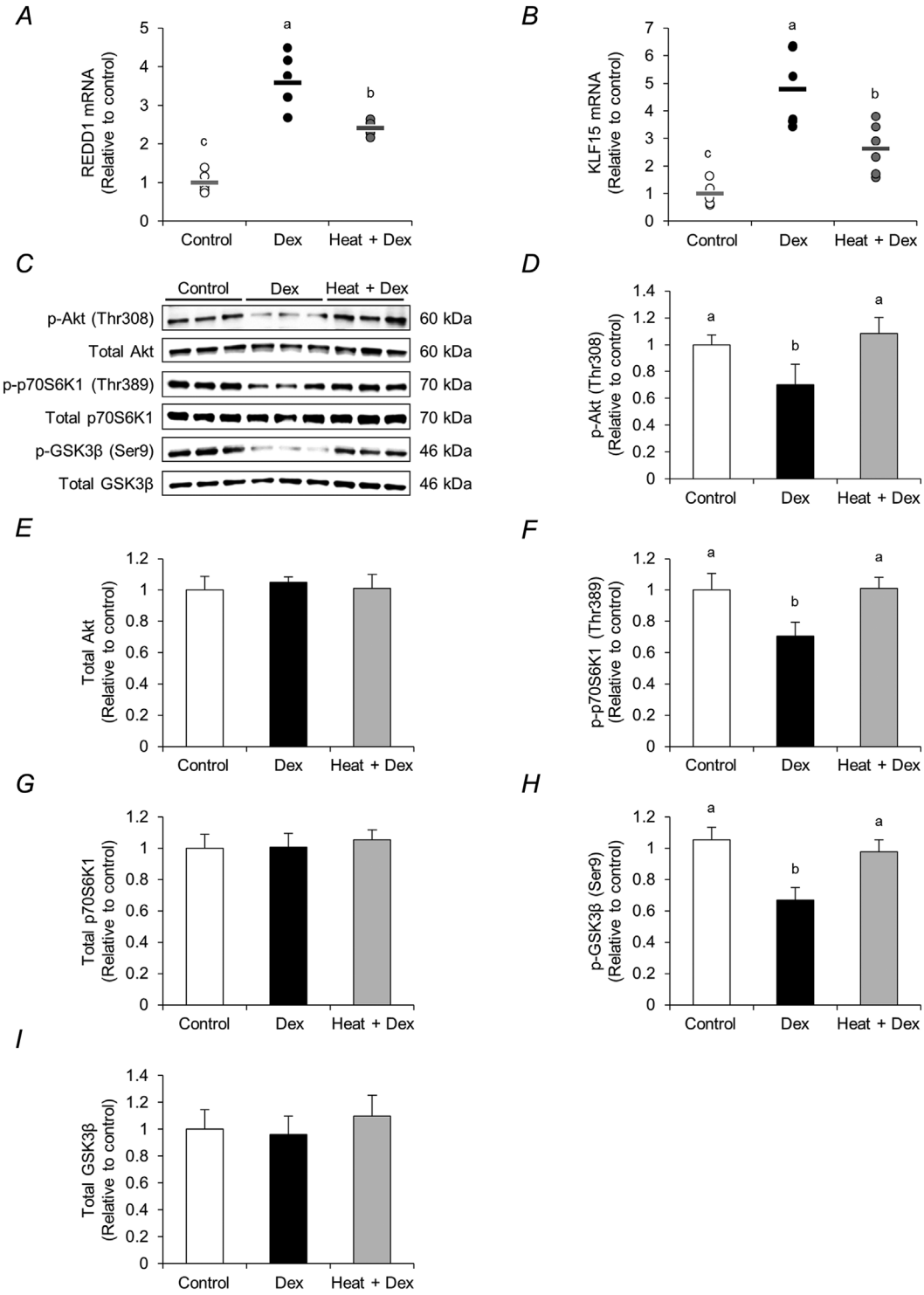


**Fig. 5. Heat stress normalizes Dex-induced increases in REDD1 and KLF15 mRNA expression and decreases in phosphorylated Akt, p70S6K1, and GSK3β. Fully differentiated C2C12 myotubes were exposed to heating (at 41°C for 60 min) 6 h prior to 10 μM Dex treatment for 3 h. The experiment was conducted using three conditions, control, Dex, and Heat + Dex, as described for Figure 3. A and B: REDD1 and KLF15 mRNA expressions were measured by real-time quantitative RT-PCR. Horizontal bars indicate mean values (n = 6 dishes per condition), relative to the mean value of the control condition that was set as 1. C–I: Levels of phosphorylated and total Akt, p70S6K1, and GSK3β were measured by western blotting and are expressed as means ± SD (n = 6 dishes per condition). a–c indicate significant differences among the designated groups ($P < 0.05$), where a > b > c.**

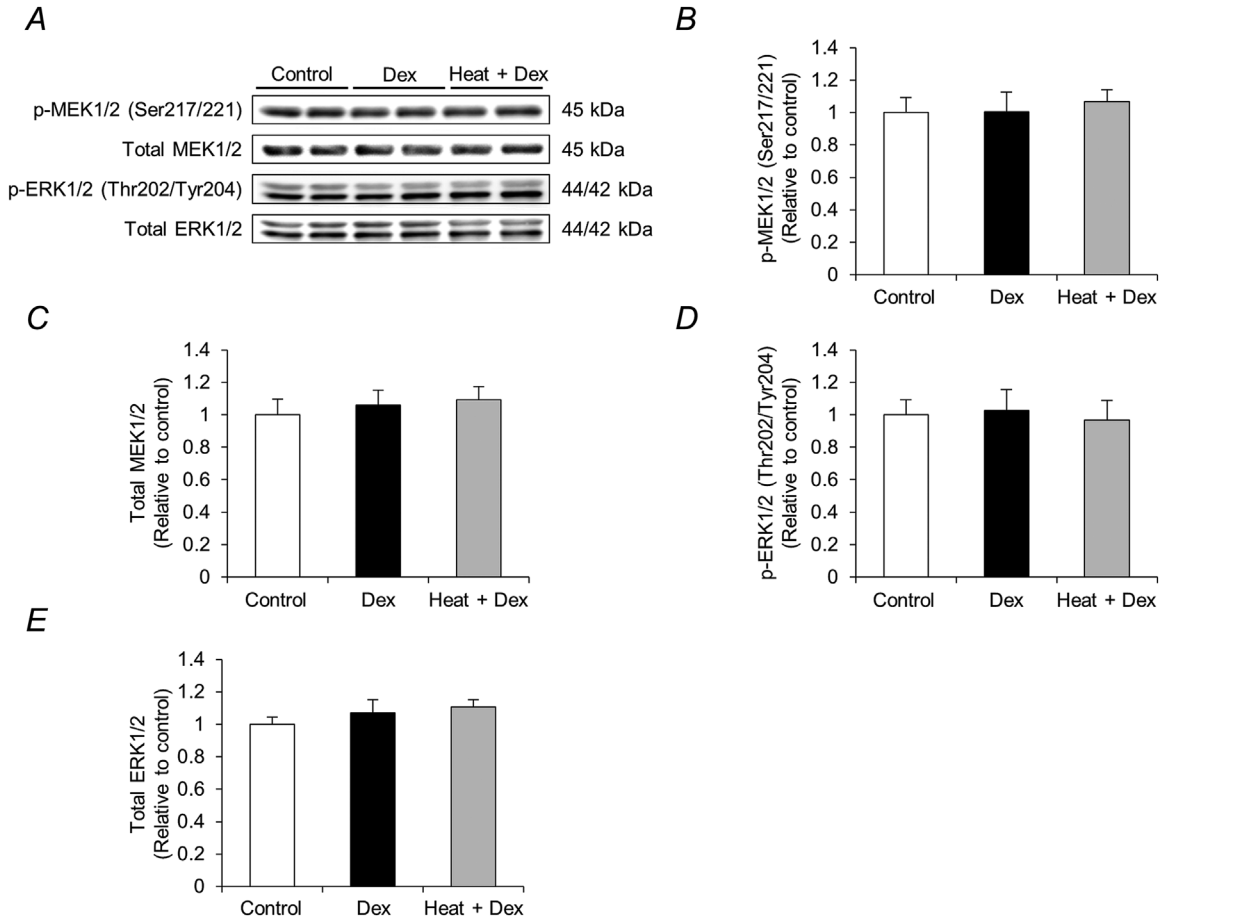


**Fig. 6. Dex treatment and heat stress do not alter the levels of phosphorylated and total MEK1/2 and ERK1/2. Fully differentiated C2C12 myotubes were exposed to heating (at 41°C for 60 min) 6 h prior to 10 μM Dex treatment for 3 h. The experiment was conducted using three conditions, control, Dex, and Heat + Dex, as described for Figure 3. A–E: Levels of phosphorylated and total MEK1/2 and ERK1/2 were measured by western blotting and are expressed as means ± SD (n = 6 dishes per condition).**

### Heat stress normalizes decreases in phosphorylated Akt, p70S6K1, and GSK3β by Dex through PI3K-dependent mechanisms

Recent studies have shown that Dex exerted anti-anabolic actions by inhibiting PI3K/Akt-dependent mTORC1 signaling (Kuo et al., 2012). To determine whether heat stress suppressed the Dex-induced inhibition of PI3K/Akt signaling, we determined basal phosphorylation status of Akt (Thr308), p70S6K1 (Thr389), and GSK3β (Ser9) in non-Dex treated myotubes with/without a PI3K inhibitor, wortmannin. Lower concentrations of wortmannin (10–100 nM) had no effect, whereas higher concentrations (0.5–10 μM) decreased phosphorylated Akt, p70S6K1, and GSK3β (Supplemental Fig. S3A–G). Therefore, 100 nM wortmannin was used for all further experiments to investigate whether PI3K is required for the heat stress suppression of Dex-induced decreases in phosphorylated Akt, p70S6K1, and GSK3β. Fully differentiated C2C12 myotubes were treated with 100 nM wortmannin 2 h before heat treatment, and then exposed to heat stress (at 41°C for 60 min) ending 6 h prior to treatment with Dex for 3 h. Wortmannin completely abolished the inhibitory effect of heat stress on Dex-induced decreases in phosphorylated Akt, p70S6K1, and GSK3β with no change in each total protein level (Fig. 7A and C–H). Therefore, heat stress may normalize the Dex-induced inhibition of anabolic pathways through PI3K-dependent mechanisms. We also confirmed that wortmannin did not inhibit the heat stress-induced increase in Hsp72 protein expression in Dex-treated C2C12 (Fig. 7A and B).

### Heat stress partially attenuates Dex-induced decreases in myotube diameter through PI3K-dependent mechanisms

Because wortmannin blocked the inhibitory effect of heat stress on Dex-induced decreases of phosphorylated Akt, p70S6K1, and GSK3β, we examined whether PI3K was required for the anti-atrophic effects of heat stress. Fully differentiated C2C12 myotubes were treated with 100 nM wortmannin 2 h before heat treatment, and were exposed to heat stress (at 41°C for 60 min) ending 6 h prior to treatment with Dex for 24 h. Wortmannin did not affect the diameter of C2C12 myotubes with/without Dex treatment (Fig. 8A and B). However, wortmannin attenuated, but did not abolish, the inhibitory effect of heat stress on Dex-induced decreases in myotube diameter (Fig. 8A and B). Therefore, heat stress may

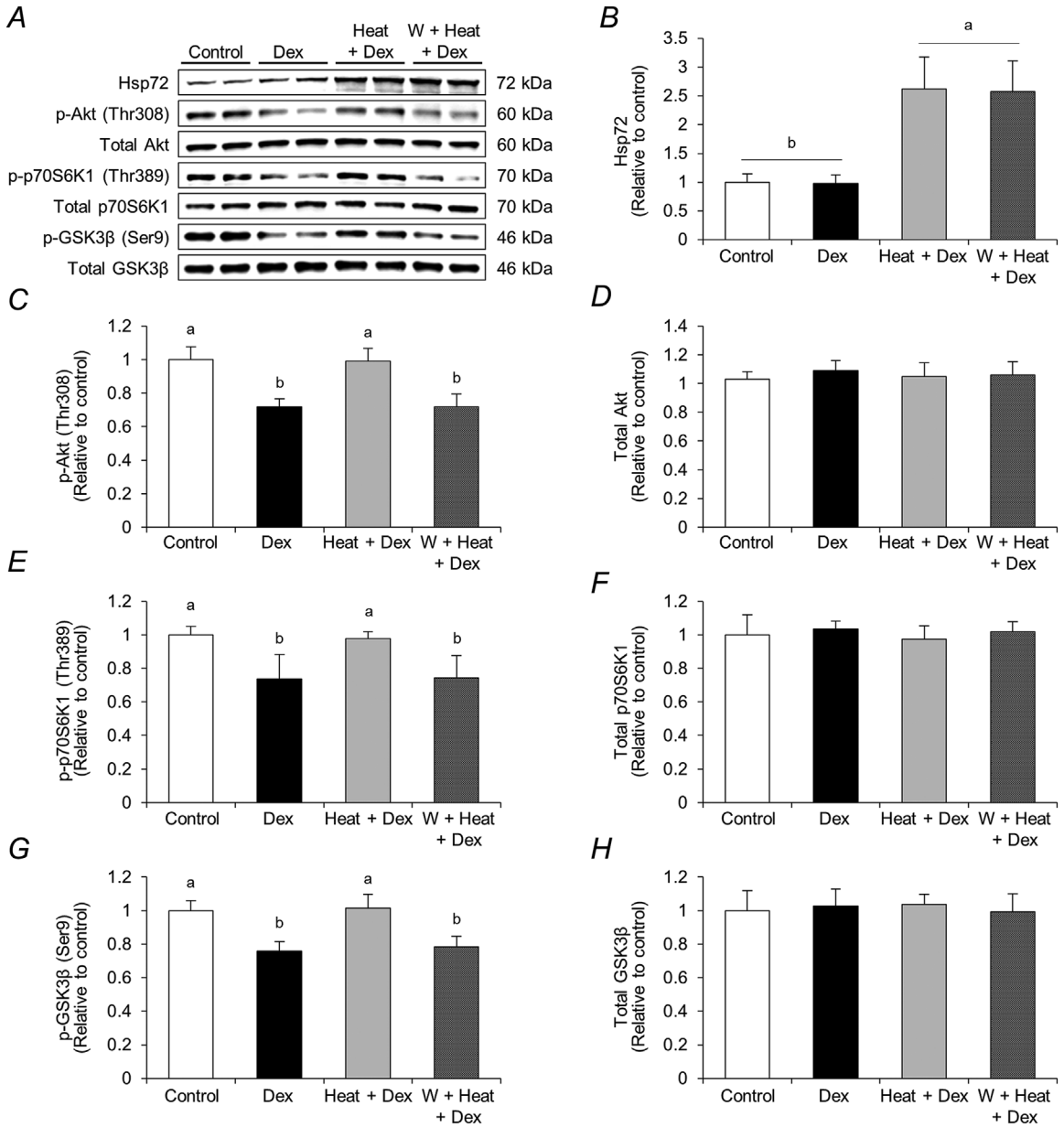


**Fig. 7. Heat stress normalizes Dex-induced decreases in phosphorylated Akt, p70S6K1, and GSK3β through PI3K-dependent mechanisms. Fully differentiated C2C12 myotubes were treated with wortmannin (100 nM) at the indicated concentrations 2 h before heat treatment, and were exposed to heating (at 41°C for 60 min) 6 h prior to 10 μM Dex treatment for 3 h. Wortmannin was maintained throughout the experiment. The experiment was conducted using four conditions, control, Dex, Heat + Dex, and wortmannin + Heat + Dex (W + Heat + Dex). A–H: Hsp72 protein expression and levels of phosphorylated and total Akt, p70S6K1, and GSK3β were measured by western blotting and are expressed as means ± SD (n = 8 dishes per condition), relative to the mean value of the control condition that was set as 1. a and b indicate significant differences among the designated groups ($P < 0.05$), where a > b.**

partially attenuate Dex-induced decreases in myotube diameter through PI3K-dependent mechanisms.

### Heat stress suppresses Dex-induced increases in KLF15 and MuRF1 mRNA expression, decreases in phosphorylated Akt, FoxO1, and FoxO3a protein levels, and increases in total FoxO1 and FoxO3a in C2C12 myotubes

Dex induces KLF15, which interacts with the promoter regions of MuRF1 and Atrogin-1 to induce their expression (Shimizu et al., 2011). Overexpression of constitutively active forms of KLF15 increased FoxO1 and FoxO3a expressions (Shimizu et al., 2011). Our results showed that KLF15 was increased 6.2-fold in C2C12 myotubes at 6 h Dex treatment (Fig. 9A), corresponding with increased total FoxO1 (1.2-fold, $P = 0.0644$) and FoxO3a (1.5-fold, $P < 0.05$) protein levels (Fig. 9B, F, and H). These increases were prevented by heat stress.

Dephosphorylation and the activation of FoxO1 and FoxO3a by dephosphorylating and inactivating Akt, resulted in MuRF1 and Atrogin-1 mRNA expression, inducing atrophy

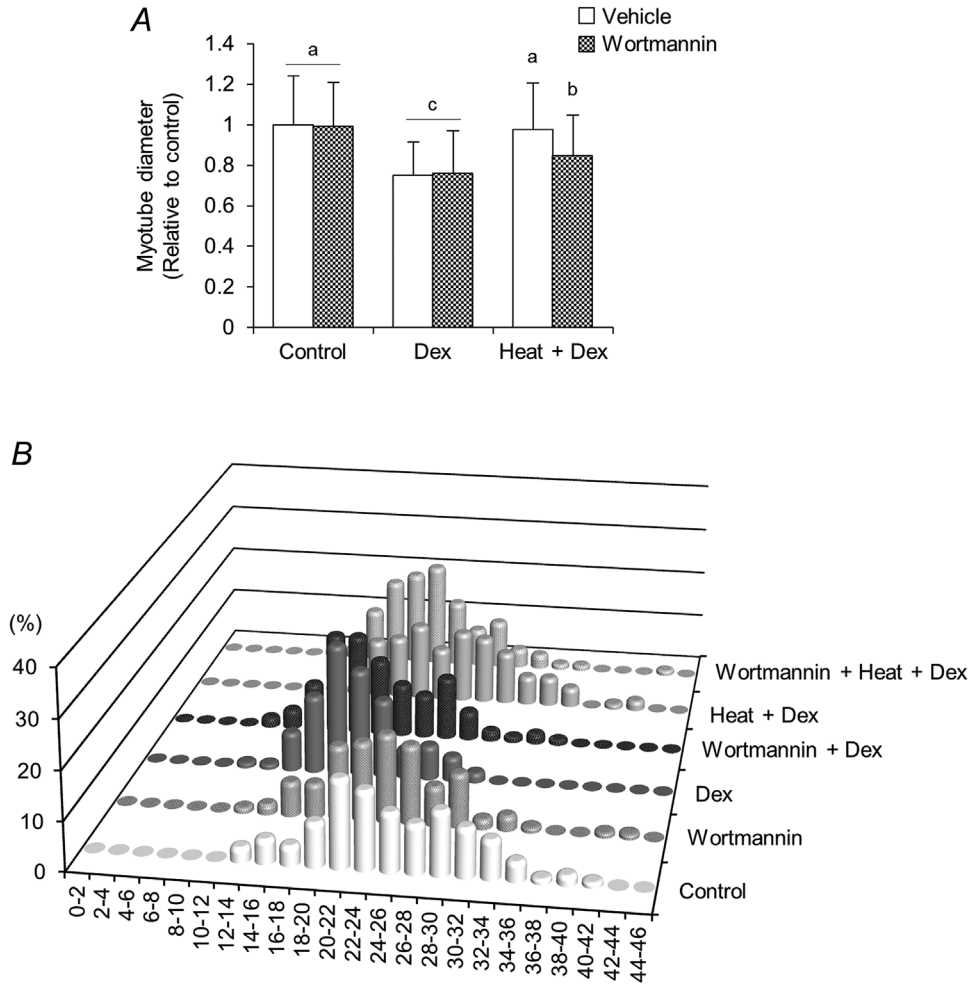


**Fig. 8. Heat stress attenuates Dex-induced decreases in myotube diameter through PI3K-dependent mechanisms. Fully differentiated C2C12 myotubes were treated with 100 nM wortmannin 2 h before heat treatment, and were exposed to heating (at 41°C for 60 min) 6 h prior to adding 10 μM Dex and treating for 24 h. Wortmannin was maintained throughout the experiment. Myotube diameters were measured. The experiment was conducted using six conditions, control, wortmannin, Dex, wortmannin + Dex, Heat + Dex, and wortmannin +Heat + Dex. A: The graph shows the average myotube diameters. Data are the means ± SD ($n \geq 110$ myotubes per condition) relative to the mean value of the control condition that was set as 1. a–c indicate significant differences among the designated groups ($P < 0.05$), where a > b > c. B: Frequency histogram showing distribution of myotube diameters.**

(Sandri et al., 2004; Stitt et al., 2004). We measured the levels of phosphorylated Akt, FoxO1, and FoxO3a in C2C12 myotubes treated with Dex for 6 h. Akt phosphorylation on Thr308 was significantly decreased (32%) (Fig. 9B–D). This was inhibited by heat stress. Dex treatment also significantly decreased the phosphorylation of FoxO1 on Ser256 (48%) and FoxO3a on Ser253 (49%), both of which were reduced by heat stress (Fig. 9B, E, and G). Because FoxO1/FoxO3a induces the expression of MuRF1 and Atrogin-1, we performed qRT-PCR and found an increased abundance of mRNA for MuRF1 (1.9-fold) and Atrogin-1 (1.6-fold) after Dex treatment. Consistent with the above results, increased MuRF1 observed in response to Dex treatment was attenuated by heat stress (Fig. 9I). However, heat stress did not block the Dex-induced increase in Atrogin-1 mRNA expression (Fig. 9J).

## Discussion

Our study provided evidence that heat stress can prevent GC-mediated muscle atrophy and the upregulation of direct target genes of GC, regulated in part, by Hsp72. These observations are clinically important because high GC levels observed in Cushing's syndrome and patients treated with corticosteroids for asthma and rheumatoid arthritis are associated with muscle wasting and weakness (Bowyer et al., 1985; Seale and Compton, 1986; Carroll and Findling, 2010; Minetto et al., 2011). Thus, our results suggest that multiple patient groups suffering from GC-dependent muscle wasting may benefit from heat stress.

In the present study, we observed REDD1 upregulation in Dex-treated myotubes concomitant with decreased Akt phosphorylation on Thr308 and p70S6K1 at the mTORC1-dependent site Thr389. Although its mechanism has not been well characterized, GC treatment (Wang et al., 2006) and/or other factors (Shoshani et al., 2002; Brugarolas et al., 2004; Lin et al., 2005; Sofer et al., 2005; DeYoung et al., 2008; Protiva et al., 2008; McGhee et al., 2009; Favier et al., 2010) might transcriptionally induce REDD1 expression and it inhibits mTORC1 signaling by promoting Akt dephosphorylation on Thr308 (Britto et al., 2014; Dennis et al., 2014). Thus, increased

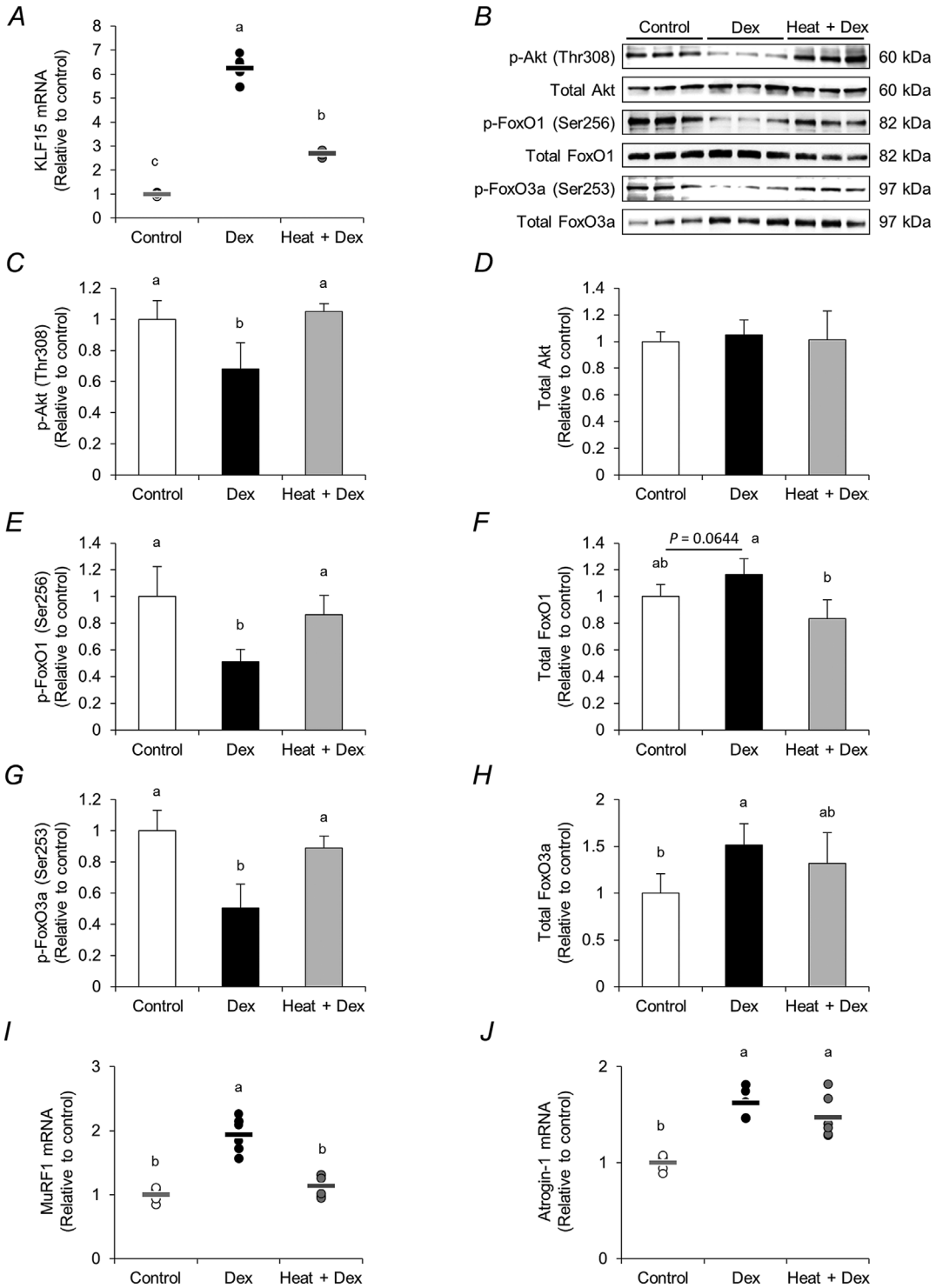


**Fig. 9. Heat stress normalizes Dex-induced increases in REDD1, MuRF1, and Atrogin-1 mRNA expressions and decreases in phosphorylated Akt, FoxO1, and FoxO3a. Fully differentiated C2C12 myotubes were exposed to heating (at 41°C for 60 min) 6 h prior to 10 μM Dex treatment for 6 h. The experiment was conducted using three conditions, control, Dex, and Heat + Dex, as described for Figure 3. A: KLF15 mRNA expression was measured by real-time quantitative RT-PCR. Horizontal bars indicate mean values (n = 6 dishes per condition), relative to the mean value of the control condition that was set as 1. B–H: Levels of phosphorylated and total Akt, FoxO1, and FoxO3a were measured by western blotting and are expressed as means ± SD (n = 6 dishes per condition). I and J: MuRF1 and Atrogin-1 mRNA expressions were measured by real-time quantitative RT-PCR. Horizontal bars indicate mean values (n = 6 dishes per condition). a–c indicate significant differences among the designated groups ($P < 0.05$), where a > b > c and ab is not different to a or b.**

REDD1 following GC treatment might hypophosphorylate Akt and p70S6K1. Furthermore, heat stress blocked Dex-induced REDD1 expression and reduction of phosphorylated Akt and p70S6K1 prevented Dex-induced muscle atrophy by suppressing mTORC1 and inhibiting protein synthesis through a mechanism involving Akt. Therefore, we propose that heat stress can exert protective effects against GC-induced muscle atrophy by inhibiting the increase in REDD1 caused by GC.

Phosphorylated Akt activates mTORC1 and inactivates GSK3β (Manning and Cantley, 2007), increasing mRNA translation initiation and subsequent protein synthesis (Proud and Denton, 1997; Ma and Blenis, 2009). Akt reduces GSK3β kinase activity by Ser9 phosphorylation, enhancing mRNA translation by increased eukaryotic translation initiation factor (eIF) 2B activity (Proud and Denton, 1997). GSK3β inhibition prevented muscle protein loss and atrophy caused by GC in vitro (Evenson et al., 2005; Fang et al., 2005; Verhees et al., 2011) and in vivo (Schakman et al., 2008), indicating muscle atrophy caused by GC was GSK3β dependent. Consistent with this, heat stress prevented the reduced phosphorylation of Akt and GSK3β and myotubular atrophy in Dex-treated C2C12 myotubes in our experiments. Thus, the prevention of Dex-mediated inhibition of GSK3β phosphorylation by heat stress reflects the normalization of phosphorylated Akt levels, and might explain how heat stress can override the anti-anabolic action of Dex in skeletal muscle.

We demonstrated PI3K was critical for the protective effects of heat stress on anabolic signaling pathways using a PI3K inhibitor. Heat stress promoted anabolic signaling in Dex-induced myotube atrophy, although heat stress-induced Akt phosphorylation at Ser308 was rapid (10 min) and transient (returned to basal levels by 60 min after heat treatment in non-Dex treated myotubes, data not shown). These data are in agreement with a recent publication by Yoshihara et al. (2016) reported in rat skeletal muscle. Thus, when investigating the protective effects of heat stress on anabolic signaling pathways, the increased effect on phosphorylated Akt may be lost in myotubes. These suggest the possibility that heat stress restores rather than stimulates PI3K/Akt signaling pathways inhibited by GC. A PI3K inhibitor also attenuated the protective effect of heat stress on Dex-induced morphological changes but did not completely abolish myotube atrophy. Thus, the anti-atrophic effects of heat stress on Dex-treated myotubes were partly mediated by the recovered PI3K/Akt signaling. Taken together, heat stress may prevent GC-induced muscle atrophy via regulating PI3K/Akt signaling pathways and modulating catabolic signaling pathways and the expression of REDD1 and KLF15 targeted by GC.

Regarding the mechanistic basis of catabolic regulation, the FoxO family of transcription factors has a pivotal role in muscle cells (Milan et al., 2015). Inhibition of insulin-like growth factor 1 (IGF1)/PI3K/Akt signaling pathway by GC dephosphorylates FoxO and mediates its nuclear transport and transactivation (Sandri et al., 2004; Stitt et al., 2004). The activation of Akt and inactivation of FoxO reduces UPS activity and decreases protein degradation (Bonaldo and Sandri, 2013). In agreement, we observed decreased phosphorylation of Akt, FoxO1, and FoxO3a in C2C12 myotubes treated with Dex, concomitant with upregulation of MuRF1 and Atrogin-1. Importantly, heat stress restored phosphorylation of Akt, FoxO1, and FoxO3a and reduced MuRF1 levels during Dex-induced muscle atrophy. Thus, the anti-atrophic effects of heat stress on Dex-treated myotubes might be mediated by the negative regulation of FoxO1/FoxO3a through the restoring phosphorylation of Akt.

A surprising finding of our study was that heat stress did not suppress Dex-induced Atrogin-1 expression, despite strongly attenuating MuRF1 mRNA expression. The reason for this is unclear but an explanation might be that MuRF1 and Atrogin-1 ubiquitinated distinct protein substrates. MuRF1 ubiquitinates muscle structural proteins, including MyHC (Clarke et al., 2007). In contrast, the identified substrates of Atrogin-1 appear to be involved in growth-related processes or survival pathways, including MyoD (Tintignac et al., 2005), a key muscle transcription factor, and eIF3F (Lagirand-Cantaloube et al., 2008), an important protein synthesis activator. Mice lacking Atrogin-1 and MuRF1 are resistant to muscle atrophy induced by denervation (Bodine et al., 2001). In contrast, Atrogin-1 knockdown prevented muscle loss during fasting (Cong et al., 2011), and MuRF1 knockout, but not Atrogin-1 knockout, mice were resistant to GC-induced muscle atrophy (Baehr et al., 2011). Therefore, MuRF1 and Atrogin-1 might not function similarly in all atrophy models and the inhibition of MuRF1 expression by heat stress may be sufficient to attenuate muscle proteolysis during GC-induced muscle atrophy, without inhibiting Atrogin-1 expression.

Interestingly, we observed that KLF15 was increased by Dex treatment, but was remarkably decreased by heat stress. KLF15 is important for amino acid catabolism and lipid utilization during skeletal muscle metabolism (Manring et al., 2014). The mechanisms by which KLF15 contributes to protein catabolism are not completely understood. Although the mechanism underlying heat stress-induced suppression of KLF15 expression in myotubes remains unclear, the beneficial effects of heat stress on muscle protein degradation and synthesis might be closely associated with the inhibition of KLF15 expression because KLF15 participates in muscle catabolism via transcriptional upregulation of FoxO1/FoxO3a, MuRF1, and Atrogin-1 (Shimizu et al., 2011) indicating KLF15 and FoxO1 cooperatively upregulate MuRF1 and Atrogin-1 expression.

It has been reported that heat stress attenuated reductions in soleus muscle mass and fiber size in various animal models (Naito et al., 2000; Selsby and Dodd, 2005), indicating Hsp72 might be protective in the heat stress-induced suppression of muscle atrophy via its molecular chaperone and protein repair functions. Other Hsp72-mediated protective mechanisms against muscle atrophy include suppression of the proteolytic signaling pathway, including FoxO. A study of C2C12 myotubes showed that Hsp72 bound to phosphorylated Akt, protecting it from dephosphorylation, thus maintaining FoxO3a in its phosphorylated, inactive state (Kukreti et al., 2013). Furthermore, atrophy of the soleus muscle was attenuated when Hsp72 overexpression abolished FoxO3a transcriptional activity in vivo (Senf et al., 2008). Hsp72 also associates directly with GR in the cytoplasm to prevent the nuclear translocation of GR (Dittmar and Pratt, 1997; Kukreti et al., 2013). We demonstrated that heat stress increased Hsp72 expression during Dex treatment of C2C12 myotubes and prevented Dex-induced myotube atrophy. Thus, heat stress-induced increases in Hsp72 might contribute to protection against Dex-induced myotube atrophy. Future studies employing in vitro and in vivo modifications of the Hsp72 gene, by gene knockout or knockdown, will enhance our understanding of the mechanism of the beneficial effects of heat stress against GC-induced muscle atrophy.

Previous studies using cultured myotubes treated with Dex used concentrations ranging from 10–50 nM (Thompson et al., 1999; Du et al., 2000) to 10–100 μM (Stitt et al., 2004; Latres et al., 2005; Clarke et al., 2007; Verhees et al., 2011; Wada et al., 2011; Kukreti et al., 2013; Wright et al., 2015). We found that C2C12 myotubes treated with Dex for 24 h exhibited a dose-dependent reduction of diameter at 0.1–100 μM Dex and that 10 μM Dex for 24 h significantly decreased myotube diameter and myofibrillar proteins (total protein, MyHC-f, and total MyHC protein levels) consistent with previous reports (Sacheck et al., 2004; Polge et al., 2011; Verhees et al., 2011; Wright et al., 2015). An in vivo rat study showed heat stress attenuated extensor digitorum longus muscle atrophy caused by Dex (Morimoto et al., 2015). In agreement, we showed that

heat stress abolished Dex-induced reductions in myotube diameters and myofibrillar protein abundance. This led us to examine the mechanisms underlying the effects of heat stress, focusing on expression of key molecules and signaling pathways involved in regulating protein synthesis and degradation in response to GC.

In conclusion, this study identified some mechanisms involved in the protective effect of heat stress, applied prior to muscle wasting, to prevent GC-induced muscle atrophy. Heat stress attenuated Dex-induced REDD1 and KLF15 mRNA expressions. Heat stress released, at least in part, Dex-induced inhibition of PI3K/Akt/mTOR signaling and myotube atrophy through PI3K-dependent mechanisms. Understanding the cellular basis of GC-induced skeletal muscle atrophy will enable the rational development of therapeutic interventions to minimize the debilitating effects of the muscle atrophic response to GC.

## Acknowledgments

The authors are grateful to Dr. Mitsuharu Okutsu (Nagoya City University, Japan) for his helpful comments, Rina Yuminamochi (Kasugai Municipal Hospital), Tomoe Kumagai (Second Narita Memorial Hospital), Masato Tanaka (Maehara Surgery Orthopedic Surgery), and Yoshita Ohno (Nagoya University, Japan) for technical assistance in performing the experiments. This work was supported, in part, by JSPS KAKENHI Grant Numbers 26870691 (WT), 26350639 (MI) from Japan Society for the Promotion of Science (JSPS), and in part by a grant from the Public Advertisement Research Project of Nihon Fukushi University.

## Literature Cited

Baehr LM, Furlow JD, Bodine SC. 2011. Muscle sparing in muscle RING finger 1 null mice: Response to synthetic glucocorticoids. J Physiol 589:4759–4776.
Bodine SC, Latres E, Baumhueter S, Lai VK, Nunez L, Clarke BA, Poueymirou WT, Panaro FJ, Na E, Dharmarajan K, Pan ZQ, Valenzuela DM, DeChiara TM, Stitt TN, Yancopoulos GD, Glass DJ. 2001. Identification of ubiquitin ligases required for skeletal muscle atrophy. Science 294:1704–1708.
Bonaldo P, Sandri M. 2013. Cellular and molecular mechanisms of muscle atrophy. Dis Model Mech 6:25–39.
Bowyer SL, LaMothe MP, Hollister JR. 1985. Steroid myopathy: Incidence and detection in a population with asthma. J Allergy Clin Immunol 76:234–242.
Braun TP, Grossberg AJ, Krasnow SM, Levasseur PR, Szumowski M, Zhu XX, Maxson JE, Knoll JG, Barnes AP, Marks DL. 2013. Cancer- and endotoxin-induced cachexia require intact glucocorticoid signaling in skeletal muscle. FASEB J 27:3572–3582.
Braun TP, Zhu X, Szumowski M, Scott GD, Grossberg AJ, Levasseur PR, Graham K, Khan S, Damaraju S, Colmers WF, Baracos VE, Marks DL. 2011. Central nervous system inflammation induces muscle atrophy via activation of the hypothalamic-pituitary-adrenal axis. J Exp Med 208:2449–2463.
Britto FA, Begue G, Rossano B, Docquier A, Vernus B, Sar C, Ferry A, Bonnieu A, Ollendorff V, Favier FB. 2014. REDD1 deletion prevents dexamethasone-induced skeletal muscle atrophy. Am J Physiol Endocrinol Metab 307:E983–E993.
Brown EJ, Beal PA, Keith CT, Chen J, Shin TB, Schreiber SL. 1995. Control of p70 s6 kinase by kinase activity of FRAP in vivo. Nature 377:441–446.
Brugarolas J, Lei K, Hurley RL, Manning BD, Reiling JH, Hafen E, Witters LA, Ellisen LW, Kaelin WG, Jr. 2004. Regulation of mTOR function in response to hypoxia by REDD1 and the TSC1/TSC2 tumor suppressor complex. Genes Dev 18:2893–2904.
Brunn GJ, Hudson CC, Sekulic A, Williams JM, Hosoi H, Houghton PJ, Lawrence JC, Jr., Abraham RT. 1997. Phosphorylation of the translational repressor PHAS-I by the mammalian target of rapamycin. Science 277:99–101.
Carroll TB, Findling JW. 2010. The diagnosis of Cushing's syndrome. Rev Endocr Metab Disord 11:147–153.
Chromiak JA, Vandenburgh HH. 1992. Glucocorticoid-induced skeletal muscle atrophy in vitro is attenuated by mechanical stimulation. Am J Physiol 262:C1471–C1477.
Clarke BA, Drujan D, Willis MS, Murphy LO, Corpina RA, Burova E, Rakhilin SV, Stitt TN, Patterson C, Latres E, Glass DJ. 2007. The E3 Ligase MuRF1 degrades myosin heavy chain protein in dexamethasone-treated skeletal muscle. Cell Metab 6:376–385.
Cong H, Sun L, Liu C, Tien P. 2011. Inhibition of atrogin-1/MAFbx expression by adenovirus-delivered small hairpin RNAs attenuates muscle atrophy in fasting mice. Hum Gene Ther 22:313–324.
Dennis MD, Coleman CS, Berg A, Jefferson LS, Kimball SR. 2014. REDD1 enhances protein phosphatase 2A-mediated dephosphorylation of Akt to repress mTORC1 signaling. Sci Signal 7:ra68.
DeYoung MP, Horak P, Sofer A, Sgroi D, Ellisen LW. 2008. Hypoxia regulates TSC1/2-mTOR signaling and tumor suppression through REDD1-mediated 14-3-3 shuttling. Genes Dev 22:239–251.
Dittmar KD, Pratt WB. 1997. Folding of the glucocorticoid receptor by the reconstituted Hsp90-based chaperone machinery. The initial hsp90.p60.hsp70-dependent step is sufficient for creating the steroid binding conformation. J Biol Chem 272:13047–13054.
Du J, Mitch WE, Wang X, Price SR. 2000. Glucocorticoids induce proteasome C3 subunit expression in L6 muscle cells by opposing the suppression of its transcription by NF-kappa B. J Biol Chem 275:19661–19666.
Evenson AR, Fareed MU, Menconi MJ, Mitchell JC, Hasselgren PO. 2005. GSK-3beta inhibitors reduce protein degradation in muscles from septic rats and in dexamethasone-treated myotubes. Int J Biochem Cell Biol 37:2226–2238.
Fang CH, Li BG, James JH, King JK, Evenson AR, Warden GD, Hasselgren PO. 2005. Protein breakdown in muscle from burned rats is blocked by insulin-like growth factor i and glycogen synthase kinase-3beta inhibitors. Endocrinology 146:3141–3149.
Favier FB, Costes F, Defour A, Bonnefoy R, Lefai E, Bauge S, Peinnequin A, Benoit H, Freyssenet D. 2010. Downregulation of Akt/mammalian target of rapamycin pathway in skeletal muscle is associated with increased REDD1 expression in response to chronic hypoxia. Am J Physiol Regul Integr Comp Physiol 298:R1659–R1666.
Goldberg AL, Tischler M, DeMartino G, Griffin G. 1980. Hormonal regulation of protein degradation and synthesis in skeletal muscle. Fed Proc 39:31–36.
Gwag T, Park K, Kim E, Son C, Park J, Nikawa T, Choi I. 2013. Inhibition of C2C12 myotube atrophy by a novel HSP70 inducer, celastrol, via activation of Akt1 and ERK1/2 pathways. Arch Biochem Biophys 537:21–30.
Hickson RC, Davis JR. 1981. Partial prevention of glucocorticoid-induced muscle atrophy by endurance training. Am J Physiol 241:E226–E232.
Hu Z, Wang H, Lee IH, Du J, Mitch WE. 2009. Endogenous glucocorticoids and impaired insulin signaling are both required to stimulate muscle wasting under pathophysiological conditions in mice. J Clin Invest 119:3059–3069.
Ichinoseki-Sekine N, Yoshihara T, Kakigi R, Sugiura T, Powers SK, Naito H. 2014. Heat stress protects against mechanical ventilation-induced diaphragmatic atrophy. J Appl Physiol 117:518–524.
Iwata M, Suzuki S, Hayakawa K, Inoue T, Naruse K. 2009. Uniaxial cyclic stretch increases glucose uptake into C2C12 myotubes through a signaling pathway independent of insulin-like growth factor I. Horm Metab Res 41:16–22.
Kadmiel M, Cidlowski JA. 2013. Glucocorticoid receptor signaling in health and disease. Trends Pharmacol Sci 34:518–530.
Kamei Y, Miura S, Suzuki M, Kai Y, Mizukami J, Taniguchi T, Mochida K, Hata T, Matsuda J, Aburatani H, Nishino I, Ezaki O. 2004. Skeletal muscle FOXO1 (FKHR) transgenic mice have less skeletal muscle mass, down-regulated Type I (slow twitch/red muscle) fiber genes, and impaired glycemic control. J Biol Chem 279:41114–41123.
Kelleher AR, Kimball SR, Dennis MD, Schilder RJ, Jefferson LS. 2013. The mTORC1 signaling repressors REDD1/2 are rapidly induced and activation of p70S6K1 by leucine is defective in skeletal muscle of an immobilized rat hindlimb. Am J Physiol Endocrinol Metab 304:E229–E236.
Kukreti H, Amuthavalli K, Harikumar A, Sathiyamoorthy S, Feng PZ, Anantharaj R, Tan SL, Lokireddy S, Bonala S, Sriram S, McFarlane C, Kambadur R, Sharma M. 2013. Muscle-specific microRNA1 (miR1) targets heat shock protein 70 (HSP70) during dexamethasone-mediated atrophy. J Biol Chem 288:6663–6678.
Kuo T, Lew MJ, Mayba O, Harris CA, Speed TP, Wang JC. 2012. Genome-wide analysis of glucocorticoid receptor-binding sites in myotubes identifies gene networks modulating insulin signaling. Proc Natl Acad Sci USA 109:11160–11165.
Lagirand-Cantaloube J, Offner N, Csibi A, Leibovitch MP, Batonnet-Pichon S, Tintignac LA, Segura CT, Leibovitch SA. 2008. The initiation factor eIF3-f is a major target for atrogin1/MAFbx function in skeletal muscle atrophy. EMBO J 27:1266–1276.
Latres E, Amini AR, Amini AA, Griffiths J, Martin FJ, Wei Y, Lin HC, Yancopoulos GD, Glass DJ. 2005. Insulin-like growth factor-1 (IGF-1) inversely regulates atrophy-induced genes via the phosphatidylinositol 3-kinase/Akt/mammalian target of rapamycin (PI3 K/Akt/mTOR) pathway. J Biol Chem 280:2737–2744.
Lehmann JF, Warren CG, Scham SM. 1974. Therapeutic heat and cold. Clin Orthop Relat Res Mar–Apr:207–245.
Lin L, Qian Y, Shi X, Chen Y. 2005. Induction of a cell stress response gene RTP801 by DNA damaging agent methyl methanesulfonate through CCAAT/enhancer binding protein. Biochemistry 44:3909–3914.
Lofberg E, Gutierrez A, Wernerman J, Anderstam B, Mitch WE, Price SR, Bergstrom J, Alvestrand A. 2002. Effects of high doses of glucocorticoids on free amino acids, ribosomes and protein turnover in human muscle. Eur J Clin Invest 32:345–353.
Luo G, Sun X, Hungness E, Hasselgren PO. 2001. Heat shock protects L6 myotubes from catabolic effects of dexamethasone and prevents downregulation of NF-kappaB. Am J Physiol Regul Integr Comp Physiol 281:R1193–1200.
Ma K, Mallidis C, Bhasin S, Mahabadi V, Artaza J, Gonzalez-Cadavid N, Arias J, Salehian B. 2003. Glucocorticoid-induced skeletal muscle atrophy is associated with upregulation of myostatin gene expression. Am J Physiol Endocrinol Metab 285:E363–371.
Manning BD, Cantley LC. 2007. AKT/PKB signaling: Navigating downstream. Cell 129:1261–1274.
Manring H, Abreu E, Brotto L, Weisleder N, Brotto M. 2014. Novel excitation-contraction coupling related genes reveal aspects of muscle weakness beyond atrophy-new hopes for treatment of musculoskeletal diseases. Front Physiol 5:37.
McGhee NK, Jefferson LS, Kimball SR. 2009. Elevated corticosterone associated with food deprivation upregulates expression in rat skeletal muscle of the mTORC1 repressor, REDD1. J Nutr 139:828–834.
Menconi M, Gonnella P, Petkova V, Lecker S, Hasselgren PO. 2008. Dexamethasone and corticosterone induce similar, but not identical, muscle wasting responses in cultured L6 and C2C12 myotubes. J Cell Biochem 105:353–364.
Milan G, Romanello V, Pescatore F, Armani A, Paik JH, Frasson L, Seydel A, Zhao J, Abraham R, Goldberg AL, Blaauw B, DePinho RA, Sandri M. 2015. Regulation of autophagy and the ubiquitin-proteasome system by the FoxO transcriptional network during muscle atrophy. Nat Commun 6:6670.
Minetto MA, Lanfranco F, Botter A, Motta G, Mengozzi G, Giordano R, Picu A, Ghigo E, Arvat E. 2011. Do muscle fiber conduction slowing and decreased levels of circulating muscle proteins represent sensitive markers of steroid myopathy? A pilot study in Cushing's disease. Eur J Endocrinol 164:985–993.
Morimoto Y, Kondo Y, Kataoka H, Honda Y, Kozu R, Sakamoto J, Nakano J, Origuchi T, Yoshimura T, Okita M. 2015. Heat treatment inhibits skeletal muscle atrophy of glucocorticoid-induced myopathy in rats. Physiol Res 64:897–905.
Naito H, Powers SK, Demirel HA, Sugiura T, Dodd SL, Aoki J. 2000. Heat stress attenuates skeletal muscle atrophy in hindlimb-unweighted rats. J Appl Physiol 88:359–363.
Polge C, Heng AE, Jarzaguet M, Ventadour S, Claustre A, Combaret L, Bechet D, Matondo M, Uttenweiler-Joseph S, Monsarrat B, Attaix D, Taillandier D. 2011. Muscle actin is polyubiquitinylated in vitro and in vivo and targeted for breakdown by the E3 ligase MuRF1. FASEB J 25:3790–3802.
Protiva P, Hopkins ME, Baggett S, Yang H, Lipkin M, Holt PR, Kennelly EJ, Bernard WI. 2008. Growth inhibition of colon cancer cells by polyisoprenylated benzophenones is associated with induction of the endoplasmic reticulum response. Int J Cancer 123:687–694.

Proud CG, Denton RM. 1997. Molecular mechanisms for the control of translation by insulin. Biochem J 328:329–341.
Ramamoorthy S, Cidlowski JA. 2013. Exploring the molecular mechanisms of glucocorticoid receptor action from sensitivity to resistance. Endocr Dev 24:41–56.
Revollo JR, Cidlowski JA. 2009. Mechanisms generating diversity in glucocorticoid receptor signaling. Ann N Y Acad Sci 1179:167–178.
Sacheck JM, Ohtsuka A, McLary SC, Goldberg AL. 2004. IGF-I stimulates muscle growth by suppressing protein breakdown and expression of atrophy-related ubiquitin ligases, atrogin-1 and MuRF1. Am J Physiol Endocrinol Metab 287:E591–601.
Sandri M, Sandri C, Gilbert A, Skurk C, Calabria E, Picard A, Walsh K, Schiaffino S, Lecker SH, Goldberg AL. 2004. Foxo transcription factors induce the atrophy-related ubiquitin ligase atrogin-1 and cause skeletal muscle atrophy. Cell 117:399–412.
Schakman O, Gilson H, Thissen JP. 2008. Mechanisms of glucocorticoid-induced myopathy. J Endocrinol 197:1–10.
Seale JP, Compton MR. 1986. Side-effects of corticosteroid agents. Med J Aust 144:139–142.
Selsby JT, Dodd SL. 2005. Heat treatment reduces oxidative stress and protects muscle mass during immobilization. Am J Physiol Regul Integr Comp Physiol 289:R134–R139.
Senf SM, Dodd SL, McClung JM, Judge AR. 2008. Hsp70 overexpression inhibits NF-kappaB and Foxo3a transcriptional activities and prevents skeletal muscle atrophy. FASEB J 22:3836–3845.
Shi H, Scheffler JM, Zeng C, Pleitner JM, Hannon KM, Grant AL, Gerrard DE. 2009. Mitogen-activated protein kinase signaling is necessary for the maintenance of skeletal muscle mass. Am J Physiol Cell Physiol 296:C1040–C1048.
Shimizu N, Yoshikawa N, Ito N, Maruyama T, Suzuki Y, Takeda S, Nakae J, Tagata Y, Nishitani S, Takehana K, Sano M, Fukuda K, Suematsu M, Morimoto C, Tanaka H. 2011. Crosstalk between glucocorticoid receptor and nutritional sensor mTOR in skeletal muscle. Cell Metab 13:170–182.
Shoshani T, Faerman A, Mett I, Zelin E, Tenne T, Gorodin S, Moshel Y, Elbaz S, Budanov A, Chajut A, Kalinski H, Kamer I, Rozen A, Mor O, Keshet E, Leshkowitz D, Einat P, Skaliter R, Feinstein E. 2002. Identification of a novel hypoxia-inducible factor 1-responsive gene, RTP801, involved in apoptosis. Mol Cell Biol 22:2283–2293.
Sofer A, Lei K, Johannessen CM, Ellisen LW. 2005. Regulation of mTOR and cell growth in response to energy stress by REDD1. Mol Cell Biol 25:5834–5845.
Stefanovsky V, Langlois F, Gagnon-Kugler T, Rothblum LI, Moss T. 2006. Growth factor signaling regulates elongation of RNA polymerase I transcription in mammals via UBF phosphorylation and r-chromatin remodeling. Mol Cell 21:629–639.
Stitt TN, Drujan D, Clarke BA, Panaro F, Timofeyva Y, Kline WO, Gonzalez M, Yancopoulos GD, Glass DJ. 2004. The IGF-1/PI3K/Akt pathway prevents expression of muscle atrophy-induced ubiquitin ligases by inhibiting FOXO transcription factors. Mol Cell 14:395–403.
Tamura Y, Kitaoka Y, Matsunaga Y, Hoshino D, Hatta H. 2015. Daily heat stress treatment rescues denervation-activated mitochondrial clearance and atrophy in skeletal muscle. J Physiol 593:2707–2720.
Thompson MG, Thom A, Partridge K, Garden K, Campbell GP, Calder G, Palmer RM. 1999. Stimulation of myofibrillar protein degradation and expression of mRNA encoding the ubiquitin-proteasome system in C(2)C(12) myotubes by dexamethasone: Effect of the proteasome inhibitor MG-132. J Cell Physiol 181:455–461.
Tiao G, Fagan J, Roegner V, Lieberman M, Wang JJ, Fischer JE, Hasselgren PO. 1996. Energy-ubiquitin-dependent muscle proteolysis during sepsis in rats is regulated by glucocorticoids. J Clin Invest 97:339–348.
Tintignac LA, Lagirand J, Batonnet S, Sirri V, Leibovitch MP, Leibovitch SA. 2005. Degradation of MyoD mediated by the SCF (MAFbx) ubiquitin ligase. J Biol Chem 280:2847–2856.
Tomas FM, Munro HN, Young VR. 1979. Effect of glucocorticoid administration on the rate of muscle protein breakdown in vivo in rats, as measured by urinary excretion of N tau-methylhistidine. Biochem J 178:139–146.
Tsuchida W, Iwata M, Suzuki S, Bannno Y, Inoue T, Matsuo S, Asai Y. 2012. Inhibitory effect of heat stress on glucocorticoid induced skeletal muscle atrophy in relation to heat shock protein expression. J Phys Therap 29:795–782.
KJ Verhees, AM Schols, MC Kelders, CM Op den Kamp, JL van der Velden, RC. Langen, Glycogen synthase kinase-3beta is required for the induction of skeletal muscle atrophy Am J Physiol Cell Physiol 3012011; C995–C1007
Wada S, Kato Y, Okutsu M, Miyaki S, Suzuki K, Yan Z, Schiaffino S, Asahara H, Ushida T, Akimoto T. 2011. Translational suppression of atrophic regulators by microRNA-23a integrates resistance to skeletal muscle atrophy. J Biol Chem 286:38456–38465.
Waddell DS, Baehr LM, van den Brandt J, Johnsen SA, Reichardt HM, Furlow JD, Bodine SC. 2008. The glucocorticoid receptor and FOXO1 synergistically activate the skeletal muscle atrophy-associated MuRF1 gene. Am J Physiol Endocrinol Metab 295:E785–797.
Wang H, Kubica N, Ellisen LW, Jefferson LS, Kimball SR. 2006. Dexamethasone represses signaling through the mammalian target of rapamycin in muscle cells by enhancing expression of REDD1. J Biol Chem 281:39128–39134.
Welc SS, Phillips NA, Oca-Cossio J, Wallet SM, Chen DL, Clanton TL. 2012. Hyperthermia increases interleukin-6 in mouse skeletal muscle. Am J Physiol Cell Physiol 303:C455–466.
Wing SS, Goldberg AL. 1993. Glucocorticoids activate the ATP-ubiquitin-dependent proteolytic system in skeletal muscle during fasting. Am J Physiol 264:E668–676.
Wright CR, Brown EL, Ward AC, Russell AP. 2015. G-CSF treatment can attenuate dexamethasone-induced reduction in C2C12 myotube protein synthesis. Cytokine 73:1–7.
Yaffe D, Saxel O. 1977. Serial passaging and differentiation of myogenic cells isolated from dystrophic mouse muscle. Nature 270:725–727.
Yamamoto D, Maki T, Herningtyas EH, Ikeshita N, Shibahara H, Sugiyama Y, Nakanishi S, Iida K, Iguchi G, Takahashi Y, Kaji H, Chihara K, Okimura Y. 2010. Branched-chain amino acids protect against dexamethasone-induced soleus muscle atrophy in rats. Muscle Nerve 41:819–827.
Yoshihara T, Ichinoseki-Sekine N, Kakigi R, Tsuzuki T, Sugiura T, Powers SK, Naito H. 2015. Repeated exposure to heat stress results in a diaphragm phenotype that resists ventilator-induced diaphragm dysfunction. J Appl Physiol 119:1023–1031.
Yoshihara T, Kobayashi H, Kakigi R, Sugiura T, Naito H. 2016. Heat stress-induced phosphorylation of FoxO3a signalling in rat skeletal muscle. Acta Physiol (Oxf) doi: 10.1111/apha.12735. [Epub ahead of print].

## Supporting Information

Additional supporting information may be found in the online version of this article at the publisher's web-site.